张学君, 张垚垚, 刘凯,等. 锆石 U-Pb 和 Lu-Hf 同位素研究内蒙乌努格吐山斑岩型铜钼矿岩浆岩特征[J]. 岩矿测试,2022, 41(5):774-788.
ZHANG Xuejun, ZHANG Yaoyao, LIU Kai, et al. Zircon U-Pb and Lu-Hf Isotopic Dating of Magmatic Rocks in the Wunugetushan Porphyry Copper-Molybdenum Deposit, Inner Mongolia[J]. Rock and Mineral Analysis,2022,41(5):774-788.
【DOI: 10.15898/j.cnki.11-2131/td.202207180132】

锆石 U-Pb 和 Lu-Hf 同位素研究内蒙乌努格吐山斑岩型铜钼矿岩浆岩特征

张学君[1], 张垚垚[1,2*], 刘凯[1], 贺晓龙[3], 王书训[2], 贾伍慧[1], 赵泽南[4]
(1. 中国地质科学院, 北京 100037;
2. 中国地质大学(北京)地球科学与资源学院, 北京 100083;
3. 湘潭大学环境与资源学院, 湖南 湘潭 411105;
4. 河北省区域地质调查院, 河北 廊坊 065000)

摘要: 位于额尔古纳—呼伦断裂北西侧的乌努格吐山铜钼矿为一大型斑岩型铜钼矿床,矿区岩浆岩发育,为确定赋矿围岩和成矿母岩的侵位时代,探讨岩石成因,本文选择该矿床代表性的岩石样品,采用激光剥蚀多接收器电感耦合等离子体质谱法(LA-MC-ICP-MS)和激光剥蚀电感耦合等离子体质谱法(LA-ICP-MS),对岩浆岩的锆石 U-Pb 同位素和锆石 Lu-Hf 同位素进行了分析测定。研究表明:①研究区锆石稀土元素含量较高,重稀土强烈富集,具 δEu 负异常和 δCe 强正异常,稀土配分曲线具左倾特征;②不等粒二长花岗岩为赋矿围岩,锆石 $^{206}Pb/^{238}U$ 加权平均年龄为 200.96±0.88Ma(MSWD=3.0),岩体形成于早侏罗世,锆石 Lu-Hf 同位素特征表明岩浆源区为幔源物质和少量古老壳源物质的混合;③流纹质碎斑熔岩为成矿母岩,锆石 $^{206}Pb/^{238}U$ 加权平均年龄为 179.58±0.91Ma,形成于早侏罗世,锆石 Lu-Hf 同位素特征显示岩浆源区以幔源物质为主。研究结果揭示了从赋矿围岩到成矿母岩岩浆源区从壳源到幔源过渡的演化过程。

关键词: 乌努格吐山铜钼矿; LA-MC-ICP-MS; U-Pb 同位素; Lu-Hf 同位素; 岩石成因

要点:

(1) LA-MC-ICP-MS 锆石 U-Pb 年龄限定赋矿围岩和成矿母岩侵位时代均为早侏罗世。

(2) LA-ICP-MS 锆石 Lu-Hf 同位素结果指示成岩成矿物源主要为地幔物质。

(3) 锆石 U-Pb 年龄和 Lu-Hf 同位素反映了岩浆源区的演变过程。

中图分类号: O657.63 **文献标识码**: B

斑岩铜矿作为最重要的铜矿类型之一,为世界提供了 50%以上的金属铜资源[1]。自斑岩铜矿概念提出后,众多地质矿产学者对斑岩铜矿进行了大量的研究工作。前人在斑岩铜矿形成大地构造背景[2-4]、成矿斑岩特征[3-5]、斑岩铜矿与埃达克岩关系[3-4,6-7]、斑岩铜矿中金属来源[3,8]、成矿流体特征[8-9]等方面取得重大成果。研究表明,斑岩型铜(金或钼)成矿体系倾向于出现在线性的、典型的平行造山带中,它们与钙碱性岩基和火山链一起,常产于板块汇聚边缘活动俯冲带之上的岩浆弧中。斑岩铜(金或钼)成矿体系在空间上常与中性-酸性成分的同岩浆来源的钙碱性火山岩相关联。

收稿日期: 2022-07-18; **修回日期**: 2022-09-12; **接受日期**: 2022-09-20
基金项目: 中国地质调查局地质调查项目(DD20221677-2, DD20201165); 中国地质科学院基本科研业务费项目(JKY202011, JKY202004)
第一作者: 张学君,学士,高级工程师,地球化学专业。E-mail: 13521369270@163.com。
通信作者: 张垚垚,博士,高级工程师,同位素地球化学专业。E-mail: zhangyy@cags.ac.cn。

乌努格吐山斑岩型铜钼矿床位于额尔古纳—呼伦断裂北西侧(图 1),是中国东北地区最为重要的斑岩型铜钼矿床之一,也是中国探明的第四大铜钼伴生矿床。前人对该矿床的地质特征[10]、成岩成矿年代学[11-19]、岩石地球化学[14, 16-18]、围岩蚀变[20]、矿石矿物特征[20]、稳定同位素[14,16-18]、流体包裹体[14,21]等方面开展了大量的工作。其中,对围岩和成矿母岩进行了许多同位素年代学研究,包括绢云母 K-Ar 和 Ar-Ar、全岩 Rb-Sr、锆石 U-Pb 等测年方法。然而,由于前人研究时的采样对象、测试方法、实验室的标准和精度均有区别,所取得的年龄存在较大差异,进而导致对岩石成因和形成背景也存在不同的认识。本文在系统地质调查的基础上,选取了蚀变较弱的赋矿围岩不等粒二长花岗岩和成矿母岩流纹质碎斑熔岩的样品,通过 LA(MC)-ICP-MS 方法对锆石 U-Pb 同位素、微量元素和 Lu-Hf 同位素进行研究,精确限定了赋矿围岩和成矿母岩的形成时代,查明了岩浆岩的成因和源区特征。

1　地质概况

乌努格吐山斑岩型铜钼矿床大地构造位置上位于北东向额尔古纳—呼伦断裂的北西侧之额尔古纳地块西部。区域地层由老到新主要为古生代泥盆系,中生代侏罗系、白垩系,以及新生界[14](图 1)。区域构造受额尔古纳—呼伦深断裂的影响,主要构造线为北东向[11,13]。本区岩浆活动频繁,时代分为海西晚期、燕山早期和燕山晚期,而以燕山早期为最广泛[22]。

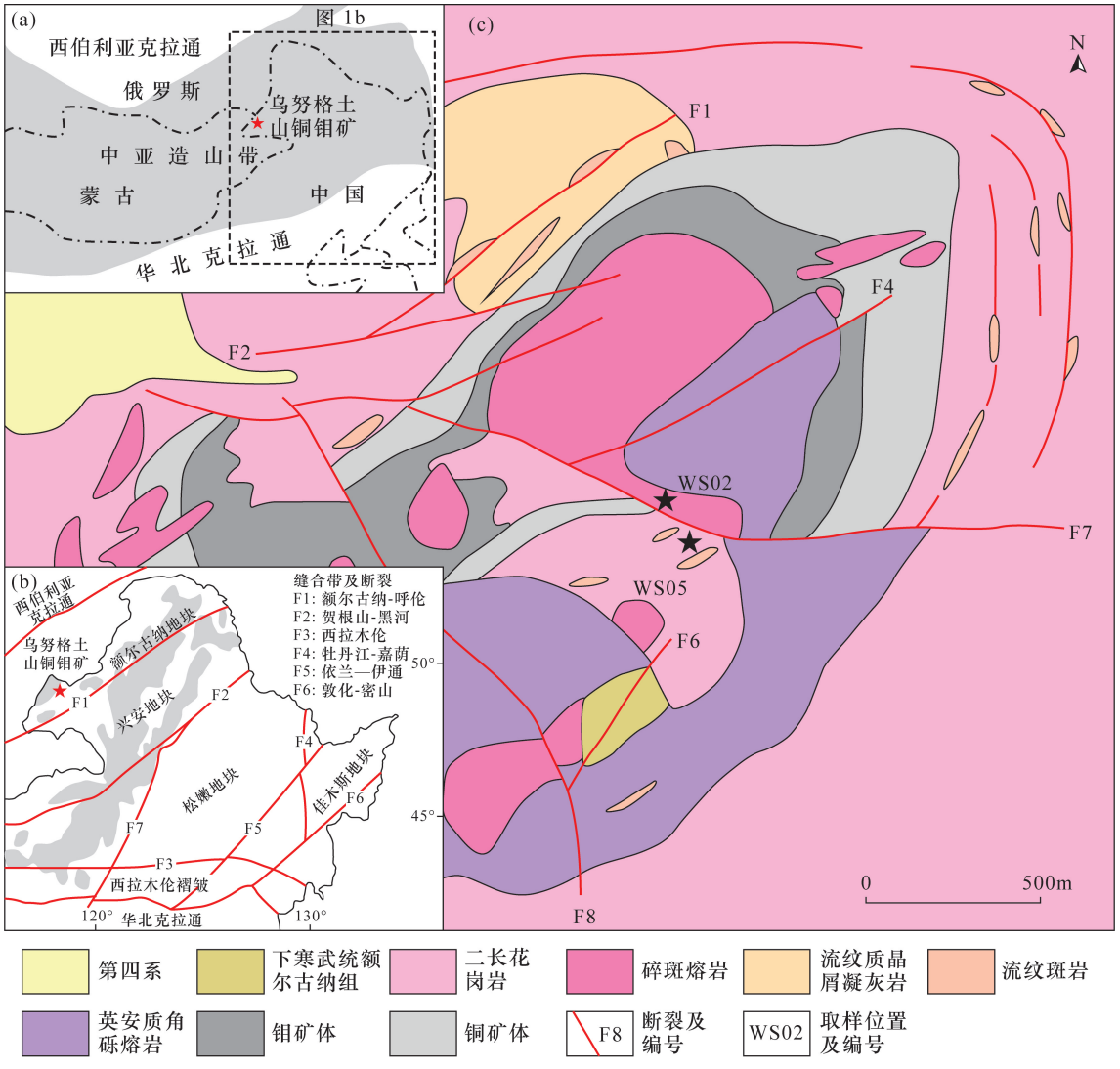

图 1　研究区(a)大地构造位置和(b)地质略图及乌努格吐山斑岩型铜钼矿床地质图(据文献[13-14,22]修改)

Fig. 1　Geotectonic location of (a) the research area, and (b) its geological sketch map, and geological map of the Wunugetushan porphyry Cu-Mo deposit (Modified after Reference [13-14,22])

矿区地层出露较为简单,主要为泥盆系上统乌奴耳组和第四系全新统,其岩性与区域上基本一致。矿区内岩浆岩较为发育,主要形成于燕山早期和燕山晚期。区域性北东向额尔古纳—呼伦深断裂位于矿区东南约 25km 处,受其影响,次一级断裂构造十分发育。赋矿围岩和成矿母岩的成岩时代及岩石成因研究可以对成矿作用有所启示。

2　实验部分

2.1　实验样品

在系统野外地质调查的基础上,结合前人在该地区的岩浆岩研究成果,选择赋矿围岩不等粒二长花岗岩(WS05)和成矿母岩流纹质碎斑熔岩(WS02)进行锆石 U-Pb 同位素和 Hf 同位素进行研究,所选取的样品较为新鲜且蚀变较弱,采样位置具体见图 1。

不等粒二长花岗岩(WS05)手标本呈显浅灰色,具不等粒花岗结构,块状构造;岩石蚀变较弱,以绿泥石化为主,并发生较弱的矿化(图 2 中 a、b)。主要组成矿物为斜长石、钾长石、石英,黑云母仅保留假像。斜长石约占 35%~45%,呈半自形-近半自形板状,粒径为 0.2~2.0mm;聚片双晶多较细密平直,为更长石,可见交代港湾结构等;常发育绢云母化、高岭土化等。钾长石约占 35%,呈近半自形板状-他形粒状,为正长石;粒径为 2~5mm,常呈杂乱状或填隙状分布,具高岭土化;粒内常见斜长石和黑云母嵌布,交代斜长石。石英约占 25%,呈他形粒状,粒内具波状、斑块状消光;呈填隙状分布于长石粒间,直径小于 5.0mm,常见集合体呈堆状聚集分布。黑云母约占 3~5%,直径小于 3.0mm,常呈叶片状零散分布,有的嵌布于钾长石粒内;发生绢云母和白云母化后常呈假像。岩石内偶见裂隙、细脉、锥状集合体发育,主要被石英、白云石、钾长石、白云母、黄铁矿、黄铜矿等矿物充填。

流纹质碎斑熔岩(WS02)手标本显浅灰色,主要为斑结构-基质霏细结构,具块状构造(图 2 中 c、d)。其中斑晶约占 40%,基质约占 60%。斑晶由长石、石英、暗色矿物构成,其中长石和暗色矿物常发

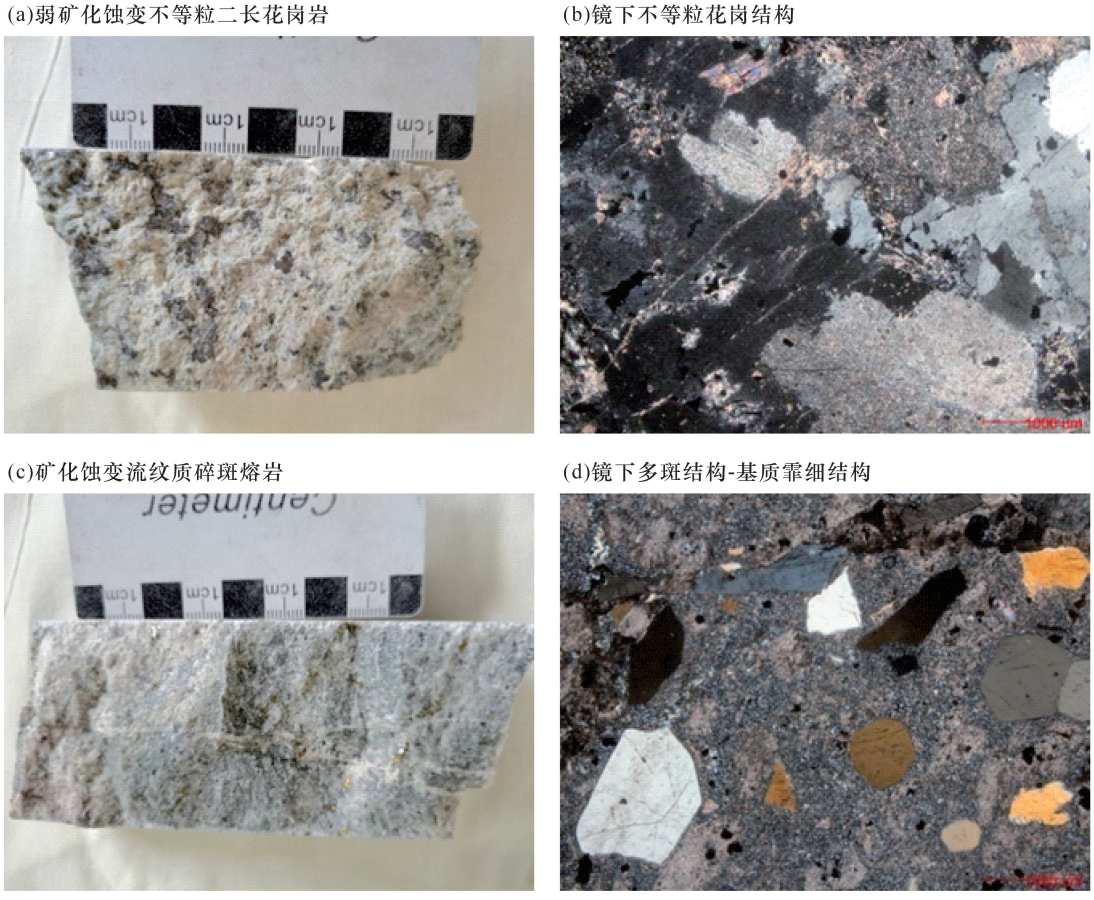

图 2　矿区围岩及成矿母岩野外与显微照片

Fig. 2　Field photos and hand specimen photograph of the surrounding rock and ore-forming parent rock

生蚀变而呈假象;粒径一般 0.1~4.5mm,略显方向性排列。长石多呈半自形-近半自形板状,较少量显棱角状、尖棱角状等,具绢云母化、少量石英化等主呈假像,局部见少量斜长石、钾长石残留,含量 35%~40%。石英多呈自形-半自形粒状,较少量显棱角状、尖棱角状,有的具熔蚀特征,含量约 15%。暗色矿物具绢云母化、白云母化等,主呈黑云母假像,少量似角闪石假像,含量 3%~5%。基质主由长英质构成。长英质具霏细结构,颗粒细小,粒径一般<0.01mm,少量 0.01~0.03mm,略具定向特征,具较明显绢云母化,含量约 45%。岩内较多见由石英、白云石、黄铁矿、黄铜矿、少量闪锌矿、白云母等充填的细脉及裂隙,另见较少量黄铁矿、黄铜矿呈星散状交代岩石。

2.2　实验方法

2.2.1　锆石 U-Pb 年龄测试

锆石的分选、制靶及透反射和阴极发光(CL)由河北省区域地质调查院实验室完成,样品经常规粉碎、磁选和重选,选出高纯度锆石,在双目镜下经人工挑选出纯度在 99%以上的锆石。将挑选好的锆石粘贴在环氧树脂表面,打磨抛光后露出锆石的表面,制成靶样。

锆石 U-Pb 年龄测试在北京锆年领航科技有限公司完成。分析仪器为 Finnigan Neptune 型 MC-ICP MS 及配套的 New Wave UP213 激光剥蚀系统,采用激光剥蚀多接收电感耦合等离子体质谱法(MC-ICP-MS)对锆石进行 U-Pb 同位素分析。激光剥蚀束斑直径为 25μm,剥蚀深度为 20~40μm,能量密度为 13~14J/cm^2,频率为 10Hz,激光剥蚀物以氦为载气进入 Neptune,利用动态变焦扩大色散可以同时接收质量数相差较大的 U-Pb 同位素。采用 Plešovice(年龄为 337±0.37Ma)[23] 作为外标样进行基体校正,普通铅校正采用 ComPbCorr#3.17 校正程序[24]。信号较小的^{207}Pb、^{206}Pb、^{204}Pb($^{+204}$Hg)、^{202}Hg 用离子计数器(multi-ion-counters)接收,^{208}Pb、^{232}Th、^{238}U 信号用法拉第杯接收,实现了所有目标同位素信号的同时接受。对采集的数据采用中国地质大学(武汉)刘勇胜博士研发的 ICP-MS DataCal 程序和 Kenneth R. Ludwig 的 Isoplot 程序进行处理,并绘制谐和图等图件,置信度为 95%。详细的仪器操作条件和数据处理方法见文献[25]。

2.2.2　锆石 Lu-Hf 年龄测试

锆石 Hf 同位素测试在北京锆年领航科技有限公司完成。锆石 Hf 同位素分析测试工作通过激光剥蚀电感耦合等离子体质谱法(LA-ICP-MS)进行。激光剥蚀系统为美国 NewWave 公司生产的 UP193FX 型 193nm ArF 准分子系统,激光器来自于德国 ATL 公司,ICP-MS 仪器型号为 Agilent 7500a。激光器波长为 193nm,脉冲宽度<4ns,束斑直径为 35μm。采用锆石标样 91500[^{176}Hf/^{177}Hf=0.282308±12(2σ)]作为外标样进行基体校正[26]。Hf 的地幔模式年龄计算中,亏损地幔^{176}Hf/^{177}Hf 值现在值采用 0.28325,^{176}Lu/^{177}Hf 值采用 0.0384[27],地壳模式年龄计算时采用平均地壳的^{176}Lu/^{177}Hf=0.015[28]。数据计算和处理采用 ICP-MS DataCal 程序完成[25]。

3　结果与讨论

3.1　锆石 U-Pb 同位素特征

用于测试的锆石自形程度较好,多为长柱状,整体较完整,发育震荡环带,具岩浆成因特征[29]。选择不发育裂隙和包裹体的锆石进行年龄测试,在发育震荡环带的位置测试(图 3 中 a、c)。

弱矿化蚀变不等粒二长花岗岩(WS05)锆石 Pb 含量为 8.17×10^{-6}~105.40×10^{-6},Th 含量为 60.44×10^{-6}~988.45×10^{-6},U 含量为 177.56×10^{-6}~2090.24×10^{-6};矿化蚀变流纹质碎斑熔岩(WS02)锆石 Pb 含量为 6.63×10^{-6}~38.32×10^{-6},Th 含量为 90.78×10^{-6}~701.01×10^{-6},U 含量为 106.28×10^{-6}~575.53×10^{-6}(表 1)。Th/U 比值均大于 0.1,为岩浆成因锆石[30-31]。样品 U-Pb 年龄<1.0Ga,因而采用锆石^{206}Pb/^{238}U 年龄[32]。WS05 样品锆石^{206}Pb/^{238}U 年龄值为 197.19±1.32~203.63±1.38Ma,加权平均值为 200.96±0.88Ma,MSWD=3.0(图 3b);WS02 样品锆石^{206}Pb/^{238}U 年龄值为 175.31±1.46~183.89±1.29Ma,加权平均值为 179.58±0.91Ma,MSWD=2.7(图 3d)。表明两类岩体均形成于早侏罗世。

3.2　锆石稀土元素特征

两类岩体锆石的稀土含量较高,弱矿化蚀变不等粒二长花岗岩(WS05)的 ΣREE 为 1036.03×10^{-6}~3489.37×10^{-6},轻稀土 LREE 含量为 13.76×10^{-6}~158.11×10^{-6},重稀土 HREE 含量为 1022.28×10^{-6}~3415.31×10^{-6},轻/重稀土比值为 0.01~0.09;矿化蚀变流纹质碎斑熔岩(WS02)的 ΣREE 为 579.83×10^{-6}~1110.14×10^{-6}(表 2),轻稀土 LREE 含量为 28.83×10^{-6}~85.54×10^{-6},重稀土 HREE 含量为 535.47×10^{-6}~1049.04×10^{-6},轻/重稀土比值为

表 1　乌努格吐山岩体 LA-MC-ICP-MS 锆石 U-Pb 同位素分析结果

Table 1　LA-MC-ICP-MS zircon U-Pb isotopic analysis of the Wunugetushan rocks

样品名	元素含量($\times10^{-6}$)			Th/U	元素比值						年龄(Ma)					
	Pb	Th	U		$^{207}Pb/^{206}Pb$	1σ	$^{207}Pb/^{235}U$	1σ	$^{206}Pb/^{238}U$	1σ	$^{207}Pb/^{206}Pb$	1σ	$^{207}Pb/^{235}U$	1σ	$^{206}Pb/^{238}U$	1σ
WS02-1	6.63	99.33	106.28	0.93	0.054800689	0.002451556	0.21777954	0.009825907	0.028920427	0.0002901	466.71	99.99	200.06	8.19	183.79	1.82
WS02-2	21.18	360.70	357.46	1.01	0.052139056	0.001611966	0.19929428	0.005904684	0.027904962	0.0002414	300.06	70.36	184.53	5.00	177.42	1.51
WS02-3	9.71	127.12	187.62	0.68	0.053187486	0.001725981	0.20737534	0.006527215	0.028589719	0.0002581	344.50	74.07	191.35	5.49	181.72	1.62
WS02-4	23.29	335.12	435.58	0.77	0.0523526	0.001072423	0.2014723	0.00400281	0.028002268	0.0001724	301.91	46.29	186.37	3.38	178.03	1.08
WS02-5	8.61	90.78	183.57	0.49	0.055145614	0.001930204	0.21747196	0.007653397	0.028658462	0.0002537	416.72	77.77	199.80	6.38	182.15	1.59
WS02-6	20.64	291.00	376.00	0.77	0.054660963	0.001447771	0.2124608	0.005765492	0.028240433	0.0002631	398.20	59.25	195.62	4.83	179.53	1.65
WS02-8	8.18	135.96	138.07	0.98	0.054630817	0.002674734	0.20791517	0.009586314	0.028118499	0.0003531	398.20	109.25	191.80	8.06	178.76	2.21
WS02-9	26.43	382.25	491.17	0.78	0.052954664	0.000994737	0.20600679	0.003891296	0.028261949	0.000183	327.84	42.59	190.20	3.28	179.66	1.15
WS02-10	10.38	130.90	207.45	0.63	0.049377333	0.001784532	0.18873552	0.006546347	0.027953044	0.0002377	164.90	87.95	175.55	5.59	177.72	1.49
WS02-11	22.22	300.23	410.94	0.73	0.052497602	0.001023893	0.20769834	0.004161734	0.028732664	0.0001882	305.62	44.44	191.62	3.50	182.61	1.18
WS02-12	38.32	701.01	575.53	1.22	0.050521629	0.000821741	0.19443142	0.003348741	0.027897904	0.0001672	220.44	34.25	180.40	2.85	177.38	1.05
WS02-13	15.41	248.04	256.19	0.97	0.050553309	0.001345129	0.19415114	0.005059312	0.02803746	0.0002147	220.44	56.47	180.17	4.30	178.25	1.35
WS02-14	16.30	256.91	298.04	0.86	0.050617744	0.001296767	0.19604288	0.004959068	0.028254753	0.0002041	233.40	59.25	181.77	4.21	179.62	1.28
WS02-15	9.86	128.93	197.58	0.65	0.053200153	0.001778239	0.20301776	0.006439848	0.027963384	0.0002068	344.50	75.92	187.68	5.44	177.79	1.30
WS02-16	11.93	159.19	228.39	0.70	0.051343842	0.001688606	0.20303925	0.006728144	0.028755703	0.0002669	257.47	71.29	187.69	5.68	182.76	1.67
WS02-17	23.68	362.75	419.53	0.86	0.054711601	0.001166784	0.21235292	0.00470457	0.028205027	0.0002095	466.71	50.92	195.53	3.94	179.30	1.31
WS02-18	10.80	134.97	212.47	0.64	0.055085188	0.00186445	0.21549537	0.007139035	0.028663977	0.0002485	416.72	80.55	198.15	5.96	182.18	1.56
WS02-19	22.29	417.16	350.97	1.19	0.051618269	0.002041641	0.19860798	0.007722468	0.02798546	0.0002789	333.39	95.36	183.95	6.54	177.93	1.75
WS02-21	28.22	505.10	401.58	1.26	0.053629164	0.001209577	0.20969736	0.004457275	0.028636014	0.0002611	353.76	51.85	193.30	3.74	182.01	1.64
WS02-22	13.76	199.73	247.98	0.81	0.050498539	0.001704943	0.19981518	0.007007338	0.028780503	0.0003232	216.74	47.22	184.97	5.93	182.91	2.03
WS02-23	15.67	233.95	279.27	0.84	0.053609854	0.001945143	0.20426492	0.006872007	0.027979173	0.0002475	353.76	50.92	188.73	5.79	177.89	1.55
WS02-24	12.13	155.47	242.85	0.64	0.048139881	0.001435921	0.18517718	0.005419974	0.028059585	0.0002194	105.65	70.37	172.51	4.64	178.39	1.38
WS02-25	21.94	294.47	456.44	0.65	0.05015908	0.001703097	0.18973048	0.006066855	0.027568544	0.0002324	211.19	79.62	176.40	5.18	175.31	1.46
WS02-26	11.03	202.63	163.39	1.24	0.048642808	0.001868937	0.18622353	0.007027353	0.028034949	0.0002515	131.57	90.73	173.40	6.02	178.24	1.58
WS02-27	18.79	270.47	307.16	0.88	0.0592801	0.001671102	0.23539905	0.006493675	0.02893611	0.0002062	575.96	58.32	214.65	5.34	183.89	1.29
WS02-28	15.65	205.15	290.46	0.71	0.050701322	0.001279128	0.20087159	0.005146519	0.028781368	0.0002166	227.85	57.40	185.86	4.35	182.92	1.36
WS02-29	17.27	254.50	308.03	0.83	0.051600767	0.001357782	0.19851122	0.005220095	0.028089674	0.0002205	333.39	61.10	183.87	4.42	178.58	1.38
WS02-30	15.90	246.27	276.75	0.89	0.051720434	0.001294036	0.19826738	0.004938912	0.027877092	0.0001995	272.29	57.40	183.66	4.19	177.25	1.25
WS05-1	64.67	982.05	957.01	1.03	0.049821594	0.000679027	0.21445247	0.003309532	0.031186237	0.0002163	187.12	31.48	197.28	2.77	197.97	1.35
WS05-2	57.13	549.94	1168.26	0.47	0.051369046	0.00067504	0.22227668	0.003450735	0.031302054	0.0002225	257.47	29.63	203.80	2.87	198.69	1.39
WS05-3	47.18	434.72	1006.50	0.43	0.0506981	0.000730666	0.2174262	0.003523028	0.031061297	0.0002109	227.85	33.33	199.77	2.94	197.19	1.32

（续表 1）

样品名	元素含量（×10⁻⁶）			Th/U	元素比值						年龄（Ma）					
	Pb	Th	U		$^{207}Pb/^{206}Pb$	1σ	$^{207}Pb/^{235}U$	1σ	$^{206}Pb/^{238}U$	1σ	$^{207}Pb/^{206}Pb$	1σ	$^{207}Pb/^{235}U$	1σ	$^{206}Pb/^{238}U$	1σ
WS05-4	34.20	444.49	539.30	0.82	0.050076452	0.00089561	0.21978911	0.003838643	0.031905458	0.0002253	198.23	36.10	201.73	3.20	202.46	1.41
WS05-5	27.24	293.62	512.29	0.57	0.050704918	0.000898261	0.2223234	0.004083565	0.03180311	0.0002221	227.85	73.14	203.84	3.39	201.82	1.39
WS05-6	36.62	406.81	627.91	0.65	0.053227511	0.000811598	0.23413474	0.003583162	0.031928406	0.0001706	338.95	35.18	213.61	2.95	202.61	1.07
WS05-7	83.00	979.16	1509.58	0.65	0.050594466	0.00081154	0.21775243	0.003377792	0.031220547	0.0001736	233.40	37.03	200.04	2.82	198.18	1.09
WS05-8	32.42	390.91	580.70	0.67	0.050650678	0.000990998	0.21692246	0.004238077	0.031130835	0.000211	233.40	72.21	199.35	3.54	197.62	1.32
WS05-9	29.94	328.98	562.17	0.59	0.052125927	0.000943859	0.22710559	0.004118635	0.031673079	0.0002015	300.06	40.74	207.81	3.41	201.01	1.26
WS05-11	44.07	450.63	852.34	0.53	0.050493385	0.000603843	0.22279877	0.002627975	0.03205128	0.000192	216.74	32.40	204.24	2.18	203.37	1.20
WS05-12	11.55	105.13	237.06	0.44	0.051080959	0.001477309	0.22439572	0.00633483	0.032046799	0.0002526	242.66	66.66	205.56	5.25	203.35	1.58
WS05-14	42.65	589.47	697.76	0.84	0.05127644	0.001010592	0.22059852	0.004252904	0.031231933	0.000197	253.77	46.29	202.41	3.54	198.25	1.23
WS05-15	39.70	446.39	683.49	0.65	0.052426052	0.001056312	0.23066064	0.004658531	0.031933659	0.0002448	305.62	46.29	210.74	3.84	202.64	1.53
WS05-16	30.83	351.35	540.24	0.65	0.05575571	0.001034747	0.24554158	0.004129216	0.032092859	0.0002217	442.64	8.33	222.95	3.37	203.63	1.38
WS05-17	31.36	393.76	522.41	0.75	0.050483307	0.001147105	0.22167031	0.004880911	0.031926872	0.0002473	216.74	84.25	203.30	4.06	202.60	1.54
WS05-18	105.40	988.45	2090.24	0.47	0.055715982	0.000922293	0.2396987	0.003938731	0.031188268	0.0002232	442.64	4.63	218.17	3.23	197.98	1.40
WS05-19	41.50	594.60	650.78	0.91	0.052764976	0.000837416	0.22901688	0.00383827	0.031430675	0.0001724	320.43	35.18	209.39	3.17	199.50	1.08
WS05-20	32.81	439.05	545.05	0.81	0.050598044	0.001078644	0.22137187	0.004978527	0.031761313	0.0002199	233.40	80.54	203.05	4.14	201.56	1.37
WS05-21	35.38	283.00	748.80	0.38	0.053983443	0.000743583	0.23800768	0.003481432	0.031971686	0.0002069	368.57	63.88	216.79	2.86	202.88	1.29
WS05-22	28.57	328.62	500.85	0.66	0.050519726	0.001050105	0.22322756	0.004803931	0.032029526	0.0002293	220.44	48.14	204.59	3.99	203.24	1.43
WS05-23	42.59	608.47	643.73	0.95	0.049834093	0.000955096	0.22053286	0.004450034	0.032048558	0.0002182	187.12	44.44	202.35	3.70	203.36	1.36
WS05-24	8.17	60.44	177.56	0.34	0.052461445	0.001898692	0.22941335	0.00798765	0.032038934	0.0002929	305.62	83.33	209.71	6.60	203.30	1.83
WS05-25	24.90	213.14	529.34	0.40	0.053206234	0.000909342	0.23360332	0.004100044	0.031832937	0.0002027	344.50	38.89	213.17	3.37	202.01	1.27
WS05-26	30.48	333.52	561.03	0.59	0.050610366	0.00098056	0.22392893	0.004444282	0.032039082	0.0001895	233.40	78.69	205.17	3.69	203.30	1.18
WS05-27	42.92	359.80	939.57	0.38	0.053112655	0.000673233	0.23125454	0.003331502	0.031536009	0.0002358	344.50	27.78	211.23	2.75	200.15	1.47
WS05-28	24.77	245.33	487.82	0.50	0.05240212	0.001044812	0.23207116	0.004988243	0.032062634	0.0002458	301.91	44.44	211.91	4.11	203.44	1.54
WS05-29	88.23	961.68	1634.70	0.59	0.051403159	0.000521454	0.22632576	0.00277416	0.03194678	0.0002878	257.47	24.07	207.16	2.30	202.72	1.80
WS05-30	45.76	621.40	772.57	0.80	0.050900004	0.00083911	0.21961879	0.00358115	0.03129567	0.0001579	235.25	37.03	201.59	2.98	198.65	0.99

表 2　锆石稀土元素($\times10^{-6}$)组成

Table 2　REE element ($\times10^{-6}$) compositions of the zircons

样品编号	La	Ce	Pr	Nd	Sm	Eu	Gd	Tb	Dy	Ho	Er	Tm	Yb	Lu	Y	ΣREE	LREE	HREE	LREE/HREE	δEu	δCe
WS05-1	0.009	30.818	0.109	2.207	5.808	1.336	37.462	14.819	189.182	78.302	365.255	82.336	775.232	155.907	2317.566	1738.78	40.29	1698.50	0.02	0.28	243.55
WS05-2	0.136	31.651	0.383	3.864	6.669	0.940	38.640	16.064	209.545	91.003	450.613	107.613	1082.980	229.910	2788.147	2270.01	43.64	2226.37	0.02	0.18	33.96
WS05-4	0.033	26.488	0.276	4.746	10.352	3.109	61.401	22.084	281.410	113.924	528.866	118.980	1130.763	227.279	3457.657	2529.71	45.00	2484.71	0.02	0.38	68.45
WS05-5	1.985	26.801	0.971	5.922	5.631	1.404	38.216	15.136	206.981	89.074	430.765	100.296	995.993	206.695	2738.920	2125.87	42.71	2083.16	0.02	0.29	4.73
WS05-6	7.588	48.479	4.041	22.978	9.309	1.237	35.817	12.572	166.430	71.866	347.266	81.181	817.296	167.611	2167.755	1793.67	93.63	1700.04	0.06	0.21	2.15
WS05-7	0.410	34.403	0.259	2.745	5.160	0.656	36.139	14.704	194.596	81.371	391.476	88.285	871.715	179.856	2485.255	1901.77	43.63	1858.14	0.02	0.15	25.90
WS05-8	0.071	26.437	0.180	3.754	6.534	1.671	45.710	17.406	241.011	104.037	496.093	114.322	1096.435	226.859	3098.375	2380.52	38.65	2341.87	0.02	0.30	57.53
WS05-9	0.634	19.833	0.405	4.501	6.978	1.302	43.246	15.843	207.008	86.747	414.299	94.644	940.131	191.090	2642.584	2026.66	33.65	1993.01	0.02	0.23	9.60
WS05-11	0.132	22.938	0.122	1.732	3.547	0.468	29.152	11.791	165.304	72.780	361.164	85.935	859.033	177.858	2241.112	1791.96	28.94	1763.02	0.02	0.14	44.37
WS05-12	0.004	8.790	0.057	1.131	3.136	0.640	19.128	7.017	97.977	41.175	206.170	48.490	497.626	104.694	1221.775	1036.03	13.76	1022.28	0.01	0.25	138.94
WS05-14	0.009	32.244	0.147	2.820	7.772	2.330	55.584	21.225	286.814	119.502	561.039	124.996	1187.688	245.743	3612.210	2647.91	45.32	2602.59	0.02	0.34	212.89
WS05-15	21.426	79.810	7.266	36.278	11.865	1.461	39.927	13.963	180.198	75.958	375.290	87.983	872.939	179.036	2355.693	1983.40	158.11	1825.29	0.09	0.21	1.57
WS05-16	0.293	20.491	0.259	4.083	8.775	1.680	49.344	17.701	216.112	87.518	406.557	90.786	878.944	176.341	2581.778	1958.88	35.58	1923.30	0.02	0.25	18.24
WS05-17	0.010	21.905	0.154	2.594	6.575	1.483	39.647	15.071	197.835	83.773	397.977	91.152	885.319	176.519	2547.626	1920.01	32.72	1887.29	0.02	0.28	133.88
WS05-18	0.236	45.705	0.646	6.351	8.428	0.844	47.397	19.589	265.616	113.368	545.382	128.379	1250.060	255.596	3519.237	2687.60	62.21	2625.39	0.02	0.13	28.68
WS05-19	0.106	31.726	0.695	12.497	23.102	5.938	113.735	37.357	433.393	165.370	720.022	158.983	1491.171	295.277	4901.935	3489.37	74.06	3415.31	0.02	0.35	28.69
WS05-20	0.018	21.968	0.154	2.858	6.418	1.727	45.681	17.085	223.461	92.612	432.575	100.645	974.587	198.240	2787.431	2118.03	33.14	2084.89	0.02	0.31	103.06
WS05-21	0.004	21.146	0.046	1.445	3.019	0.626	24.090	10.259	142.687	63.075	325.911	77.391	790.708	167.260	1970.759	1627.67	26.29	1601.38	0.02	0.22	407.07
WS05-22	0.009	21.816	0.142	3.198	6.343	1.554	41.438	15.424	207.699	87.686	414.011	96.134	937.960	194.215	2622.130	2027.63	33.06	1994.57	0.02	0.29	151.73
WS05-23	0.003	22.911	0.098	1.891	3.940	1.176	29.171	11.371	149.383	61.629	293.179	65.118	632.896	128.904	1849.730	1401.67	30.02	1371.65	0.02	0.34	316.29
WS05-25	0.002	16.515	0.045	1.028	3.357	0.484	23.728	10.029	137.925	61.334	312.802	75.410	763.433	161.320	1887.306	1567.41	21.43	1545.98	0.01	0.17	393.39
WS05-26	1.008	24.326	0.398	2.601	4.114	0.720	25.298	9.861	133.470	56.062	278.105	65.256	647.789	133.518	1756.502	1382.53	33.17	1349.36	0.02	0.22	9.41
WS05-27	0.092	25.471	0.132	1.488	3.234	0.412	22.485	9.565	134.435	59.983	305.314	76.238	761.997	161.823	1859.903	1562.67	30.83	1531.84	0.02	0.15	56.82
WS05-28	0.003	18.423	0.075	1.262	3.754	0.691	25.768	9.865	134.315	59.939	296.515	71.285	712.008	147.629	1821.177	1481.53	24.21	1457.32	0.02	0.21	300.82
WS05-29	0.004	35.127	0.083	1.768	4.805	0.560	36.981	14.534	195.832	83.381	406.337	94.943	902.927	182.187	2596.732	1959.47	42.35	1917.12	0.02	0.13	476.84
WS05-30	0.036	28.599	0.176	3.424	7.606	1.394	51.304	19.131	240.823	97.181	453.263	101.128	968.755	193.054	2897.227	2165.87	41.24	2124.64	0.02	0.22	88.05
WS02-1	0.012	34.124	0.201	3.717	7.501	2.472	33.922	10.145	110.736	40.545	175.905	38.370	354.954	72.500	1190.890	885.10	48.03	837.08	0.06	0.47	171.62

（续表 2）

样品编号	La	Ce	Pr	Nd	Sm	Eu	Gd	Tb	Dy	Ho	Er	Tm	Yb	Lu	Y	ΣREE	LREE	HREE	LREE/HREE	δEu	δCe
WS02-2	0.004	47.559	0.028	0.832	1.807	0.754	11.337	3.437	45.540	19.866	103.023	26.165	283.910	69.933	671.635	614.20	50.98	563.21	0.09	0.51	1098.02
WS02-3	0.036	38.471	0.057	1.129	1.884	0.852	13.736	4.517	57.026	24.387	123.912	31.368	334.975	77.953	794.007	710.30	42.43	667.87	0.06	0.51	208.54
WS02-4	0.012	50.641	0.028	0.917	2.720	1.204	23.208	8.413	108.997	44.986	213.779	49.899	493.407	105.741	1389.597	1103.95	55.52	1048.43	0.05	0.46	663.38
WS02-5	0.028	25.975	0.035	0.491	1.696	0.609	9.999	3.803	50.945	22.719	116.668	30.012	320.913	76.685	716.429	660.58	28.83	631.74	0.05	0.45	204.19
WS02-6	0.002	39.230	0.043	1.074	1.639	0.847	14.867	5.382	65.972	26.461	127.859	29.241	297.651	61.893	825.531	672.16	42.83	629.32	0.07	0.52	1165.23
WS02-8	0.022	49.184	0.100	1.682	4.625	1.492	25.052	8.713	107.265	41.207	186.206	42.565	411.247	85.181	1270.296	964.54	57.11	907.44	0.06	0.42	255.34
WS02-10	0.037	39.545	0.062	0.682	1.360	0.751	9.690	3.256	44.980	21.913	123.529	33.255	385.436	97.691	775.348	762.19	42.44	719.75	0.06	0.63	201.55
WS02-11	0.021	50.670	0.048	0.923	3.155	1.071	21.971	7.807	103.572	42.221	202.132	45.845	453.713	95.438	1281.416	1028.59	55.89	972.70	0.06	0.39	393.96
WS02-12	0.058	79.046	0.052	1.273	3.551	1.560	23.297	8.214	102.291	40.931	194.555	45.875	471.126	105.613	1292.794	1077.44	85.54	991.90	0.09	0.52	351.83
WS02-13	0.007	41.369	0.031	0.585	1.481	0.882	10.855	3.720	45.719	19.385	103.144	24.923	266.428	61.299	660.738	579.83	44.36	535.47	0.08	0.67	678.70
WS02-14	0.090	42.582	0.057	0.907	2.388	0.960	15.585	5.242	67.882	29.502	146.837	35.601	377.324	83.402	952.952	808.36	46.98	761.37	0.06	0.48	145.43
WS02-15	0.001	36.232	0.025	0.652	1.487	0.687	10.554	3.614	47.289	21.155	108.615	27.361	292.008	67.054	706.786	616.73	39.08	577.65	0.07	0.53	1613.59
WS02-16	0.006	34.544	0.034	0.576	1.889	0.791	11.415	3.799	49.643	20.958	111.258	28.462	308.290	73.409	720.434	645.07	37.84	607.23	0.06	0.52	592.69
WS02-17	0.019	55.315	0.094	1.178	3.093	1.401	22.447	8.198	105.758	43.429	211.144	49.744	502.611	105.706	1372.515	1110.14	61.10	1049.04	0.06	0.51	317.77
WS02-18	0.114	33.968	0.085	0.792	2.304	0.919	14.432	5.286	72.123	29.318	141.600	33.361	341.146	71.884	906.553	747.33	38.18	709.15	0.05	0.49	84.73
WS02-21	3.329	70.750	0.675	4.084	2.962	1.097	16.614	5.693	71.338	29.382	145.671	35.768	374.958	86.700	942.341	849.02	82.90	766.12	0.11	0.48	11.57
WS02-22	0.016	34.745	0.029	0.489	1.662	0.649	11.137	3.800	52.177	22.416	116.877	28.201	305.484	70.054	710.722	647.73	37.59	610.14	0.06	0.46	403.25
WS02-23	0.107	62.564	0.076	1.118	2.358	1.186	17.166	6.850	88.307	38.545	193.851	47.299	498.511	118.403	1243.373	1076.34	67.41	1008.93	0.07	0.57	170.98
WS02-24	2.004	48.432	0.640	3.362	2.621	0.843	14.286	5.148	70.194	31.348	160.890	41.314	434.070	97.581	1022.773	912.73	57.90	854.83	0.07	0.42	10.48
WS02-26	0.005	46.151	0.095	1.871	5.035	1.709	25.118	7.616	91.112	34.882	155.620	35.799	330.432	66.691	1025.318	802.14	54.87	747.27	0.07	0.46	517.34
WS02-27	2.028	56.031	0.752	4.134	4.097	1.387	22.082	7.776	94.715	39.040	181.422	42.463	422.544	89.574	1187.650	968.05	68.43	899.62	0.08	0.45	11.12
WS02-28	0.008	47.547	0.023	0.658	2.307	0.831	14.808	5.122	69.094	31.174	158.314	38.944	424.423	95.861	1005.799	889.11	51.37	837.74	0.06	0.43	873.10
WS02-29	0.032	49.428	0.052	0.873	2.233	1.023	17.366	6.285	84.980	36.660	184.098	44.561	457.590	101.390	1191.673	986.57	53.64	932.93	0.06	0.50	297.46
WS02-30	0.004	59.507	0.064	0.916	2.714	1.230	17.426	6.273	80.858	35.278	178.230	44.319	468.570	107.968	1157.665	1003.36	64.43	938.92	0.07	0.55	961.76

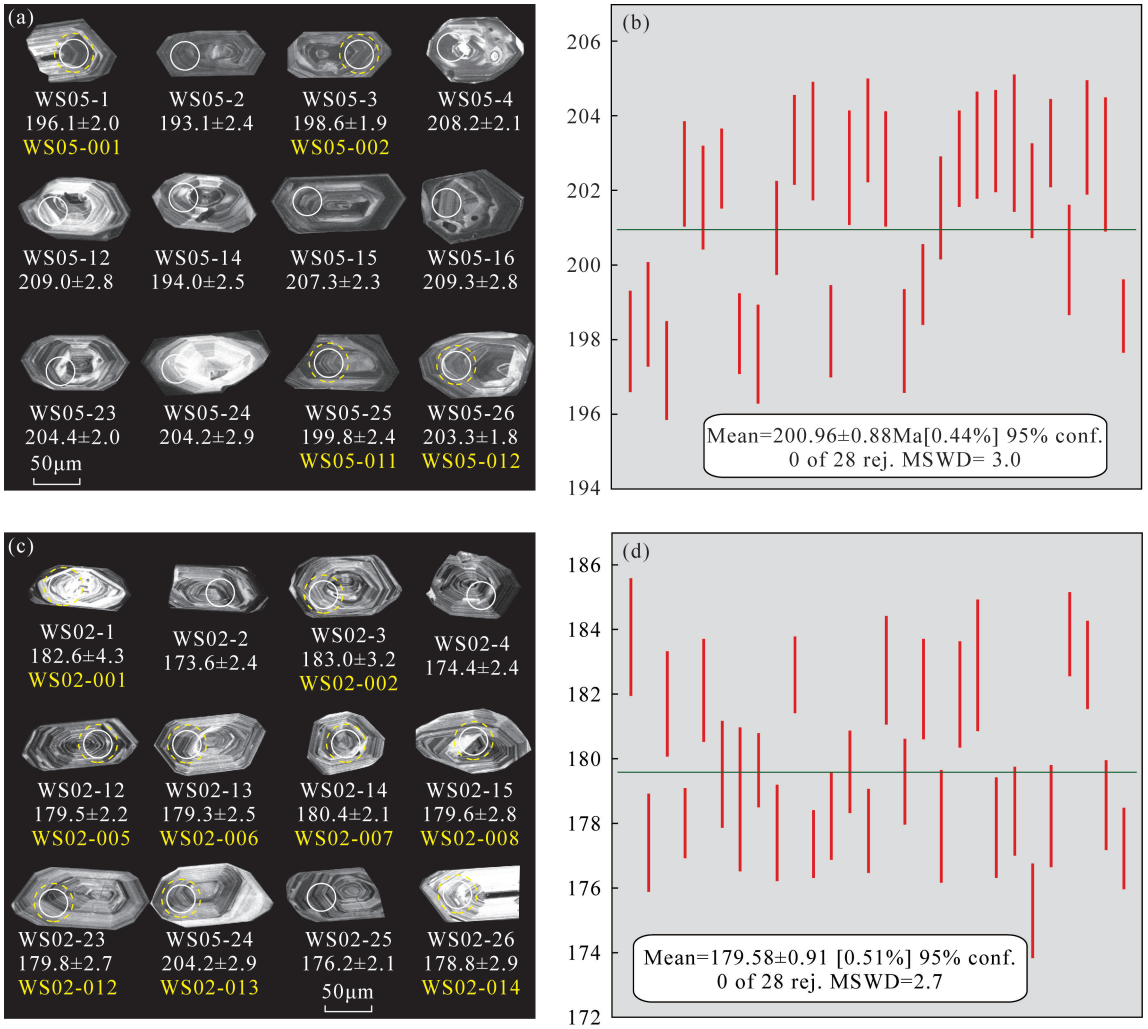

图 3　矿区围岩及成矿母岩锆石 CL 图像及年龄图

Fig. 3　Zircon CL images and age maps of surrounding rocks and ore-forming parent rocks in the mining area

0.05~0.11。轻重稀土分异程度较高,具岩浆锆石稀土元素特征[33-35]。WS05 样品锆石 δEu 值为 0.13~0.38,WS02 样品 δEu 值为 0.39~0.67,具负异常;WS05 样品锆石 δCe 值为 1.57~476.84,WS02 样品 δCe 值为 10.48~1613.59,具强正异常,与典型热液锆石差异较大[36]。两类岩体锆石稀土配分曲线具左倾特征,轻稀土亏损、重稀土富集,具岩浆锆石特征(图 4)。

3.3　锆石 Lu-Hf 同位素特征

弱矿化蚀变不等粒二长花岗岩(WS05)、矿化蚀变流纹质碎斑熔岩(WS02)锆石$^{176}Lu/^{177}Hf$ 比值分别为 0.001688~0.003588、0.000831~0.001292,$^{176}Lu/^{177}Hf$ 比值均较小,表明锆石在形成后,仅具有少量的放射性成因 Hf 积累,因而可以用初始$^{176}Hf/^{177}Hf$ 比值代表形成时的 Hf 同位素组成[37]。$^{176}Hf/^{177}Hf$ 初始比值和 $\varepsilon_{Hf}(t)$ 值根据同一锆石 U-Pb 测年数据计算;二阶段模式年龄(T_{DM}^{C})根据亏损幔源计算[27]。测定结果显示,WS05 锆石 Hf 同

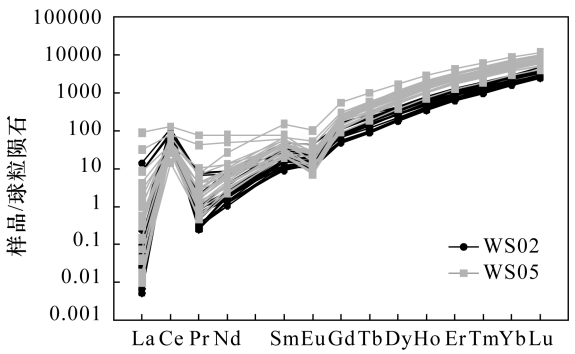

图 4　稀土元素球粒陨石标准化配分型式(标准化数据据文献[38])

Fig. 4　Chondrite-normalized REE patterns (Normalization values after Reference [38])

位素$^{176}Hf/^{177}Hf$ 比值为 0.282659 ~ 0.282820(表 3),$^{176}Yb/^{177}Hf$ 比值为 0.099606~0.046370,$f_{Lu/Hf}$ 为-0.95~-0.89,锆石 $\varepsilon_{Hf}(0)$ 为-4.0~-0.7,$\varepsilon_{Hf}(t)$ 为 0.1~5.8(图 5);WS02 锆石 Hf 同位素$^{176}Hf/^{177}Hf$ 比值为 0.282783 ~ 0.282850,$^{176}Yb/^{177}Hf$ 比值为 0.020042~0.035646,$f_{Lu/Hf}$ 为-0.97~-0.96,锆石 $\varepsilon_{Hf}(0)$ 为 0.4~2.8,$\varepsilon_{Hf}(t)$ 为 4.3~6.6(图 6)。WS05 锆石 Hf 单阶段模式年龄(T_{DM})为 643~882Ma,二阶段模式年龄(T_{DM}^{C})为 874~1235Ma;WS02 锆石 Hf 单阶段模式年龄(T_{DM})为 570~663Ma,二阶段模式年龄(T_{DM}^{C})为 802~952Ma。

3.4　成岩时代对成矿作用的约束

乌努格吐山成岩成矿年代学取得大量成果,也存在较大争议[11-15]。本次工作在系统野外地质调查的基础上,选择代表性围岩和成矿母岩进行同位素年龄测试,测试单位为北京锆年领航科技有限公司,测试方法为 LA-ICP-MS。锆石 U-Pb 年龄具有成熟有效,锆石易挑选,封闭体系温度高等优点[39-40],所测年龄结果真实有效,能够有效地代表岩体形成年龄。

表 3　乌努格吐山岩体 LA-ICP-MS 锆石 Lu-Hf 同位素分析结果

Table 3　LA-ICP-MS Zircon Lu-Hf isotopic analysis of Wunugetushan rocks

样品编号	年龄(Ma)	$^{176}Yb/^{177}Hf$	$^{176}Lu/^{177}Hf$	$^{176}Hf/^{177}Hf$	$\varepsilon_{Hf}(0)$	$\varepsilon_{Hf}(t)$	T_{DM}(Ma)	T_{DM}^{C}(Ma)	$f_{Lu/Hf}$
WS02-001	183.79	0.035646	0.001292	0.282829	2.0	5.9	604	850	-0.96
WS02-002	181.72	0.022735	0.000914	0.282783	0.4	4.3	663	952	-0.97
WS02-003	178.76	0.023283	0.000875	0.282837	2.3	6.1	587	833	-0.97
WS02-004	177.72	0.024778	0.000996	0.282818	1.6	5.4	616	878	-0.97
WS02-005	177.38	0.030802	0.001225	0.282803	1.1	4.8	641	914	-0.96
WS02-006	178.25	0.022562	0.000964	0.282825	1.9	5.7	604	860	-0.97
WS02-007	179.62	0.020253	0.000831	0.282831	2.1	5.9	595	846	-0.97
WS02-008	177.79	0.026337	0.001096	0.282842	2.5	6.3	582	822	-0.97
WS02-009	182.76	0.022090	0.000917	0.282804	1.1	5.0	634	905	-0.97
WS02-010	182.18	0.026716	0.000988	0.282850	2.8	6.6	570	802	-0.97
WS02-011	182.91	0.023562	0.000917	0.282834	2.2	6.1	591	837	-0.97
WS02-012	177.89	0.020042	0.000854	0.282819	1.7	5.5	611	873	-0.97
WS02-013	178.39	0.026401	0.001009	0.282829	2.0	5.8	599	851	-0.97
WS02-014	178.24	0.024919	0.000902	0.282803	1.1	4.9	634	909	-0.97
WS02-015	178.58	0.027675	0.001052	0.282809	1.3	5.1	629	897	-0.97
WS02-016	177.25	0.025114	0.001094	0.282813	1.5	5.2	623	888	-0.97
WS05-001	197.97	0.067606	0.002426	0.282738	-1.2	2.8	756	1057	-0.93
WS05-002	197.19	0.060028	0.002184	0.282694	-2.8	1.3	816	1155	-0.93
WS05-003	201.82	0.073935	0.002745	0.282820	1.7	5.8	643	874	-0.92
WS05-004	202.61	0.059110	0.002155	0.282728	-1.5	2.6	765	1074	-0.94
WS05-005	197.62	0.067911	0.002509	0.282731	-1.4	2.6	768	1073	-0.92
WS05-006	201.01	0.052678	0.002027	0.282712	-2.1	2.0	786	1110	-0.94
WS05-007	203.37	0.046370	0.001688	0.282703	-2.4	1.8	792	1127	-0.95
WS05-008	199.5	0.099606	0.003588	0.282743	-1.0	2.9	775	1055	-0.89
WS05-009	201.56	0.047960	0.001782	0.282714	-2.0	2.1	778	1103	-0.95
WS05-010	202.88	0.058686	0.002184	0.282702	-2.5	1.7	805	1135	-0.93
WS05-011	202.01	0.059888	0.002143	0.282712	-2.1	2.0	789	1111	-0.94
WS05-012	203.3	0.077946	0.002817	0.282659	-4.0	0.1	882	1235	-0.92
WS05-013	200.15	0.056164	0.002059	0.282711	-2.1	2.0	788	1113	-0.94
WS05-014	202.72	0.085910	0.003052	0.282701	-2.5	1.5	825	1143	-0.91
WS05-015	198.65	0.091676	0.003159	0.282751	-0.7	3.2	753	1034	-0.90

注: $\varepsilon_{Hf}(t)=10000\times\{[(^{176}Hf/^{177}Hf)_S-(^{176}Lu/^{177}Hf)_S\times(e^{\lambda t}-1)]/[(^{176}Hf/^{177}Hf)_{CHUR,0}-(^{176}Lu/^{177}Hf)_{CHUR}\times(e^{\lambda t}-1)]-1\}$;

$T_{DM}=1/\lambda\times\ln\{1+[(^{176}Hf/^{177}Hf)_S-(^{176}Hf/^{177}Hf)_{DM}]/[(^{176}Hf/^{177}Hf)_S-(^{176}Hf/^{177}Hf)_{DM}]\}$;

$T_{DMC}=T_{DM}-(T_{DM}-t)\times[(f_{cc}-f_s)/(f_{cc}-f_{DM})]$,$f_{Lu/Hf}=(^{176}Lu/^{177}Hf)_S/(^{176}Lu/^{177}Hf)^{CHUR}-1$。

其中:$\lambda=1.867\times10^{-11}/a$[41]; $(^{176}Lu/^{177}Hf)_S$ 和 $(^{176}Hf/^{177}Hf)_S$ 为样品测量值; $(^{176}Lu/^{177}Hf)_{CHUR}=0.0332$, $(^{176}Hf/^{177}Hf)_{CHUR,0}=0.282772$[26]; $(^{176}Lu/^{177}Hf)_{DM}=0.0384$, $(^{176}Hf/^{177}Hf)_{DM}=0.28325$[27]; $(^{176}Lu/^{177}Hf)_{平均地壳}=0.015$; $f_{cc}=[(^{176}Lu/^{177}Hf)_{平均地壳}/(^{176}Lu/^{177}Hf)_{CHUR}]-1$; $f_S=f_{Lu/Hf}$; $f_{DM}=[(^{176}Lu/^{177}Hf)_{DM}/(^{176}Lu/^{177}Hf)_{CHUR}]-1$; t 为锆石结晶年龄。

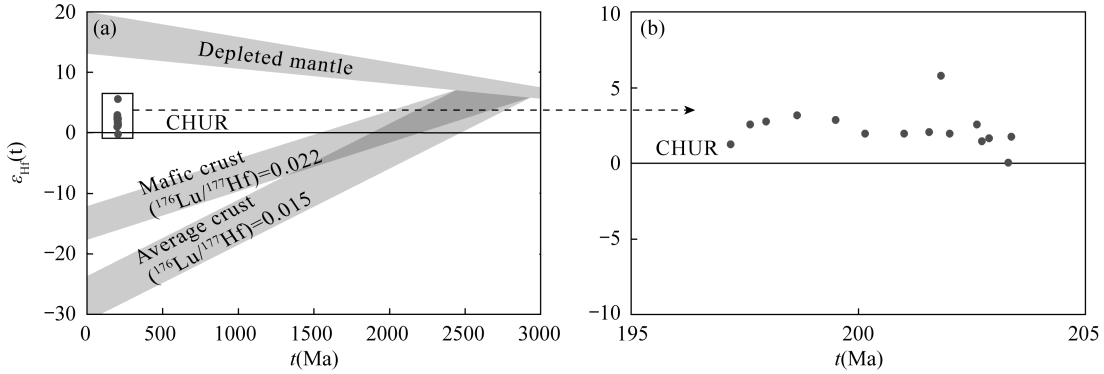

图 5　不等粒二长花岗岩(WS05)锆石 $\varepsilon_{Hf}(t)$-t 图(底图据文献[33])

Fig. 5　$\varepsilon_{Hf}(t)$ *versus* age diagrams of unequal-grained monzogranite (WS05). Base image according to Reference[33]

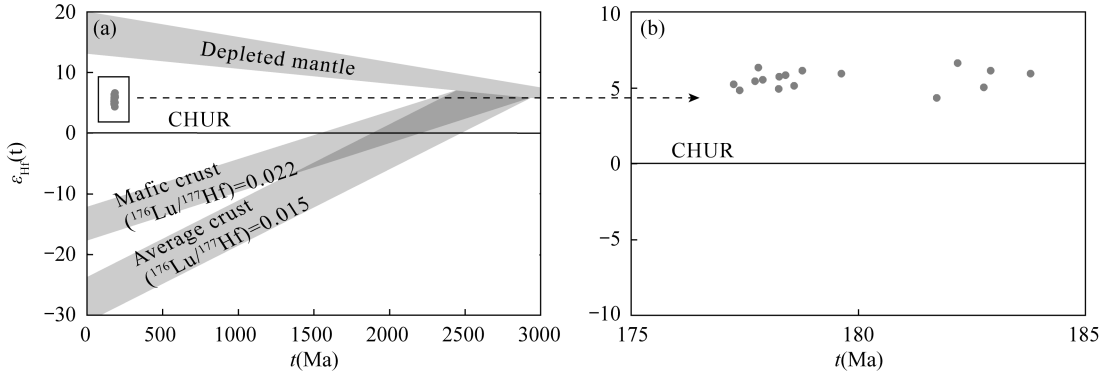

图 6　流纹质碎斑熔岩(WS02)锆石 $\varepsilon_{Hf}(t)$-t 图(底图据文献[33])

Fig. 6　$\varepsilon_{Hf}(t)$ *versus* age diagrams of rhyolite porphyritic lava (WS02). Base image according to Reference [33]

本次工作所测围岩(WS05)不等粒二长花岗岩样品锆石具震荡环带,Tu/U 比值较大,锆石稀土强烈富集重稀土、亏损轻稀土,δEu 负异常;δCe 正异常特征,表明测试用锆石为岩浆成因锆石,测试结果为 200.96±0.88Ma,该测试结果与秦克章等[12]测得的矿区黑云二长花岗岩全岩 Rb-Sr 等时线年龄(211±21Ma)、谭刚[14]获得的外围黑云母花岗岩锆石 U-Pb 年龄(198.1±2.9Ma)、Wang 等[16]获得的矿区黑云花岗岩 SIMS 锆石 U-Pb 年龄(203.5±1.6Ma)、Zhang 等[17]测得的花岗斑岩脉的 SHRIMP 锆石 U-Pb 年龄(201.4±3.1Ma)和 Mi 等[18]获得的矿区黑云母花岗岩锆石 U-Pb 年龄(206.9±1.9Ma)在误差范围内,表明了 200Ma 左右是本区重要的成岩时期,主体为大面积展布的黑云母花岗岩和二长花岗岩,其次为花岗斑岩脉体。其中,本次研究的不等粒二长花岗岩为新报道的一类赋矿围岩,与黑云母花岗岩属于同期形成的岩体在不同部位的岩性过渡。因此,本次所测得的不等粒二长花岗岩年龄(200.96±0.88Ma)可代表赋矿围岩岩体形成的时代,该岩体在靠近斑岩体的部位发育一定程度的蚀变和矿化,表明成矿作用晚于大面积展布的二长花岗岩-黑云母花岗岩围岩的形成时代。

成矿母岩(WS02)流纹质碎斑熔岩样品锆石具震荡环带,Tu/U 比值较大,锆石稀土强烈富集重稀土、亏损轻稀土,δEu 负异常;δCe 正异常特征,表明测试用锆石为岩浆成因锆石,加权平均值为 179.58±0.91Ma,表明矿化蚀变流纹质碎斑熔岩形成于早侏罗世。该测试结果与秦克章等[11]获得的蚀变绢云母 K-Ar 年龄(183.5±1.7Ma)、Wang 等[16]获得的二长花岗斑岩 SIMS 锆石 U-Pb 年龄(180.4±1.4Ma)和 Mi 等[18]获得的流纹斑岩锆石 U-Pb 年龄(180.4±4.5Ma)年龄在地质误差范围内,也与 Zhang 等[17]获得的辉钼矿 Re-Os 加权平均年龄(179.8±1.0Ma)在误差内一致,稍早于谭钢[14]测得的辉钼矿 Re-Os 等时线年龄(177.4±2.4Ma),说明除了二长花岗斑岩和流纹斑岩,本次研究的流纹质碎斑熔岩也为一种重要的成矿母岩体,其形成年龄可代表矿区的成矿时代。

赋矿围岩锆石 Hf 同位素特征表明岩浆源区以新生陆壳物质或幔源物质为主,混有少量古老壳源物质。成矿母岩锆石 Hf 同位素特征表明岩浆源区主要为新生陆壳物质或幔源物质为主,仅含极少数古老壳源物质。

4　结论

本文采用 LA-MC-ICP-MS 和 LA-ICP-MS 证实不等粒二长花岗岩和流纹质碎斑熔岩为早侏罗世不同阶段的产物。锆石 $\varepsilon_{Hf}(t)$ 值及二阶段模式年龄(T_{DM}^{C})的细微区别反映了岩浆源区的异同。通过对比赋矿围岩和成矿母岩成岩时代和 Lu-Hf 同位素之间的差异,指示了赋矿围岩岩浆源区为幔源物质和少量古老壳源物质的混合;成矿母岩岩浆源区主要为幔源物质。从赋矿围岩到成矿母岩岩浆源区幔源物质增加,壳源物质减少。

5　参考文献

[1] Kirkham R V, Sinclair W D. Porphyry copper, gold, molybdenum, tungsten, tin and siliver. Geology of Canadian mineral deposit type [J]. Geology Nation America 1995(1):421-446.

[2] Richards J P. Tectono-magmatic precursors for porphyry Cu-(Mo-Au) deposit formation[J]. Economic Geology, 2003,98:1515-1533.

[3] 侯增谦,潘小菲,杨志明,等. 初论大陆环境斑岩铜矿[J]. 现代地质,2007,21(2):173-180.
Hou Z Q, Pan X F, Yang Z M, et al. Porphyry Cu-(Mo-Au) deposits no related to oceanic-slab subduction: Examples from Chinese porphyry deposits in continental settings[J]. Geoscience, 2007, 21(2):173-180.

[4] 侯增谦. 斑岩 Cu-Mo-Au 矿床:新认识与新进展[J]. 地学前缘,2004,11(1):131-143.
Hou Z Q. Porphyry Cu-Mo-Au deposits: Some new insights and advances [J]. Earth Science Frontiers, 2004,11(1):131-143.

[5] 芮宗瑶,张洪涛,陈仁义,等. 斑岩铜矿研究中若干问题探讨[J]. 矿床地质,2006,25(4):491-505.
Rui Z Y, Zhang H T, Chen R Y, et al. An approach to some problems of porphyry copper deposits[J]. Mineral Deposits, 2006, 25(4):491-505.

[6] Oyarzun R, Ma'rquez A, Liho J, et al. Giant versus small porphyry copper deposits of Cenozoic age in northern Chile: Adakitic versus normal calc-alialine magmatism [J]. Mineralium Deposita, 2001, 36:794-798.

[7] Hou Z Q, Gao Y F, Qu X M, et al. Origin of adakitic intrusive generated during Mid-Miocene east-west extension in southern Tibet [J]. Earth and Planetary Science Letters, 2004, 220:139-155.

[8] Core D P, Kesler S E, Essene E J. Unusually Cu-rich magmas associated with giant porphyry copper deposits: Evidence from Bingham, Utah [J]. Geology, 2006, 34: 41-44.

[9] Harris A C, Kamenetsky V S, White N C, et al. Melt inclusions in veins: Linking magmas and porphyry Cu deposits[J]. Science, 2003, 302:2109-2111.

[10] 黄蕾蕾. 内蒙古乌努格吐山矿山高精度三维地质建模与评价[D]. 北京:中国地质大学(北京),2020:1-120.
Huang L L. High-precision three-dimensional geological modeling and evaluation of Unugtuishan mine in Inner Mongolia[D]. Beijing: China University of Geosciences (Beijing), 2020:1-120.

[11] 秦克章,李慧民,李伟实,等. 内蒙古乌努格吐山斑岩铜钼矿床的成岩、成矿时代[J]. 地质论评,1999,45(2):180-185.
Qin K Z, Li H M, Li W S, et al. Intrusion and mineralization ages of the Wunugetushan porphyry Cu-Mo deposit, Inner Mongolia, northwestern China [J]. Geological Review, 1999, 45(2):180-185.

[12] 秦克章,田中亮吏,李伟实,等. 满洲里地区印支期花岗岩 Rb-Sr 等时线年代学证据[J]. 岩石矿物学杂志,1998,17(3):235-240.
Qin K Z, Tian Z L L, Li W S, et al. The discovery of Indo-Sinian granites in Manzhouli area: Evidence from Rb-Sr isochrons[J]. Acta Petrologica et Mineralogica, 1998, 17(3):235-240.

[13] 李诺,陈衍景,赖勇,等. 内蒙古乌努格吐山斑岩铜钼矿床流体包裹体研究[J]. 岩石学报,2007,23(9):2177-2188.
Li N, Chen Y J, Lai Y, et al. Fluid inclusion study of the Wunugetushan porphyry Cu-Mo deposit, Inner Mongolia [J]. Acta Petrologica Sinica, 2007, 23(9):2177-2188.

[14] 谭刚. 内蒙古乌努格吐山斑岩铜钼矿床成矿作用研究[D]. 北京:中国地质科学院, 2011: 36-63.
Tan G. Study on mineralization of Unugtuishan porphyry Cu-Mo deposit, Inner Mongolia [D]. Beijing: Chinese Academy of Geological Sciences, 2011:36-63.

[15] 王天豪,张书义,孙德有,等. 满洲里南部中生代花岗岩的锆石 U-Pb 年龄及 Hf 同位素特征[J]. 世界地质,2014,33(1):26-38.
Wang T H, Zhang S Y, Sun D Y, et al. Zircon U-Pb ages and Hf isotopic characteristics of Mesozoic granitoids from southern Manzhouli, Inner Mongolia [J]. Global

Geology,2014,33(1):26-38.

[16] Wang Y H,Zhao C B,Zhang F F,et al. SIMS zircon U-Pb and molybdenite Re-Os geochronology,Hf isotope,and whole-rock geochemistry of the Wunugetushan porphyry Cu-Mo deposit and granitoids in NE China and their geological significance[J]. Gondwana Research,2015,28,1228-1245.

[17] Zhang F F,Wang Y H,Liu J J,et al. Origin of the Wunugetushan porphyry Cu-Mo deposit,Inner Mongolia,NE China:Constraints from geology,geochronology,geochemistry,and isotopic compositions[J]. Journal of Asian Earth Sciences,2016,117:208-224.

[18] Mi K F,Liu Z J,Liu R B,et al. U-Pb zircon,geochemical and Sr-Nd-Hf isotopic constraints on age and origin of the intrusions from Wunugetushan porphyry deposit,northeast China:Implication for Triassic—Jurassic Cu-Mo mineralization in Mongolia—Erguna metallogenic belt[J]. International Geology Review,2017,60(4):496-512.

[19] 宓奎峰,吕志成,柳振江,等. 内蒙古乌努格吐山铜钼矿床 Cu,Mo 同位素组成及绢云母 Ar-Ar 测年对区域成矿作用的启示[J]. 岩石学报,2021,37(6):1875-1898.
Fu K F,Lyu Z C,Liu Z J,et al. Compositions of Cu and Mo isotopes,sericite Ar-Ar ages of Wunugetushan Cu-Mo deposit in Inner Mongolia:Implications for regional mineralization[J]. Acta Petrologica Sinica,2021,37(6):1875-1898.

[20] 陈殿芬,艾永德,李荫清. 乌努格吐山斑岩铜钼矿床中金属矿物的特征[J]. 岩石矿物学杂志,1996,15(4):346-354.
Chen D F,Ai Y D,Li Y Q. Characteristics of metallic minerals from the Wunugetushan porphyry copper-molybdenum deposit[J]. Acta Petrologica et Mineralogica,1996,15(4):346-354.

[21] 李诺,孙亚莉,李晶,等. 内蒙古乌努格吐山斑岩铜钼矿辉钼矿铼锇等时线年龄及其成矿地球动力学背景[J]. 岩石学报,2007,23(11):2881-2888.
Li N,Sun Y L,Li J,et al. Molybdenite Re/Os isochron age of the Wunugetushan porphyry Cu/Mo deposit,Inner Mongolia and its implication for metallogenic geodynamics[J]. Acta Petrologica Sinica,2007,23(11):2881-2888.

[22] He X L,Yu Q Y,Liu S Y,et al. Origin of the Erdaohe Ag-Pb-Zn deposit,central Great Xing'an Range,northeast China:Constraints from fluid inclusions,zircon U-Pb geochronology,and stable isotopes[J]. Ore Geology Reviews,2021,107:104309.

[23] Sláma J,Košler J,Condon D J,et al. Plešovice zircon—A new natural reference material for U-Pb and Hf isotopic microanalysis[J]. Chemical Geology,2008,249(1-2):1-35.

[24] AndersenT. Correction of common lead in U-Pb analyses that do not report ^{204}Pb[J]. Chemical Geology,2002,192(1-2):59-79.

[25] LiuY S,Hu Z C,Zong K Q,et al. Reappraisement and refinement of zircon U-Pb isotope and trace element analyses by LA-ICP-MS[J]. Chinese Science Bulletin,2010,55:1535-1546.

[26] Goolaerts A,Mattielli N,Jong J D,et al. Hf and Lu isotopic reference values for the zircon standard 91500 by MC-ICP-MS[J]. Chemical Geology,2004,206(1-2):1-9.

[27] Griffin W L,Pearson N J,Belousova E,et al. The Hf isotope composition of cratonic mantle:LAM-MC-ICPMS analysis of zircon megacrysts in kimberlites[J]. Geochim Cosmochim Acta,2000,64:133-147.

[28] Griffin,W L,Wang X,Jackson S E,et al. Zircon geochemistry and magma mixing,SE China:Insita analysis of Hf isotopes,Tonglu and Pingtan igneous complexes[J]. Lithos,2002,61:237-269.

[29] Rubatto D,Gebauer D. Use of cathodoluminescence for U-Pb zircon dating by IOM Microprobe:Some examples form the western Alps[M]//Cathodoluminescence in Geoscience. Germany:Springer-Verlag Berlin Heidelberg,2000:373-400.

[30] Cleasson S,Vetrin V,Bayanova T,et al. U-Pb zircon ages from a Devonian carbonatite dyke,Kola peninsula,Russia:A record of geological evolution from the Archaean to the Palaeozoic[J]. Lithos,2000,51:95-108.

[31] Belousova E A,Griffin W L,O'Reilly S Y,et al. Igneous zircon:Trace element composition as an indicator of source rock type[J]. Contributions to Mineralogy and Petrology,2002,143(5):602-622.

[32] Griffin W L,Belousova E A,Shee S R. Crustal Evolution in the northern Yilarn Craton:U-Pb and Hf-isotope evidence from detrital zircons[J]. Precambrian Research,2004,131(3-4):213-282.

[33] Hoskin P W O,Kinny P D,Whborn D,et al. Indentifying accessory mineral saturation during differentiation in granitoid magmas:An integrated approach[J]. Journal of Petrology,2000,41(9):1365-1396.

[34] Rubatto D. Zircon trace element geochemistry:Partitioning with garnet and the link between U-Pb ages and

metamorphism[J]. Chemical Geology,2002,184(1-2):123-138.

[35] Hoskin P W O,Ireland T R. Rare earth element chemistry of zircon and its use as a provenance indicatior[J]. Geology,2000,28(7):627-630.

[36] Hoskin P W P. Trace-element composition of hydrothermal zircon and the alteration of hadean zircon from the Jack Hills,Australia[M]. Geochimica et Cosmochimica Acta,2005,69(3):637-648.

[37] 吴福元,李献华,郑永飞,等. Lu-Hf 同位素体系及其岩石学应用[J]. 岩石学报,2007,02:185-220.
Wu F Y,Li X H,Zheng Y F,et al. Lu-Hf isotopic systematics and their applications in petrology[J]. Acta Petrologic Sinica,2007,23(2):185-220.

[38] Sun S S,Mcdonough W F. Chemical and isotopic systematics of ocean basalts:Impications for mantle composition and processes[M]. London: Geological Society of London and Blackwell Scientific Publications,1989:313-345.

[39] Cherniak D J,Watson E B. Pb diffusion in zircon[J]. Chemical Geology,2000,172:5-24.

[40] 吴元保,郑永飞. 锆石成因矿物学研究及其对 U-Pb 年龄解释的制约[J]. 科学通报,2004,49(16):1589-1604.
Wu Y B,Zheng Y F. Zircon genetic mineralogy and its constraints on the interpretation of U-Pb age[J]. Chinese Science Bulletin,2004,49(16):1589-1604.

[41] Söderlund U,Patchett P J,Vervoort J D,et al. The ^{176}Lu decay constant determined by Lu-Hf and U-Pb isotope systematic of Precambrian mafic intrusions[J]. Earth and Planetary Science Letters,2004,219:311-324.

Zircon U-Pb and Lu-Hf Isotopic Dating of Magmatic Rocks in the Wunugetushan Porphyry Copper-Molybdenum Deposit, Inner Mongolia

ZHANG Xuejun[1], *ZHANG Yaoyao*[1,2*], *LIU Kai*[1], *HE Xiaolong*[3], *WANG Shuxun*[2], *JIA Wuhui*[1], *ZHAO Zenan*[4]

(1. Chinese Academy of Geological Sciences, Beijing 100037, China;
2. School of Earth Sciences and Resources, China University of Geosciences (Beijing), Beijing 100083, China;
3. School of Environment and Resources, Xiangtan University, Xiangtan 411105, China;
4. Hebei Regional Geological Survey Institute, Langfang 065000, China)

HIGHLIGHTS

(1) The zircons U-Pb ages from LA-MC-ICP-MS constrain that the emplacement ages of the surrounding rock and ore-forming parent rock of the Wunugetushan copper-molybdenum deposit are early Jurassic.

(2) The zircons Lu-Hf isotopic results from LA-ICP-MS indicate that the source of ore minerals is mainly mantle-derived.

(3) The zircons U-Pb ages and Lu-Hf isotopes reflect the evolution of the magma source.

ABSTRACT

BACKGROUND: The Wunugetushan copper-molybdenum deposit located in the northwest of the Erguna—Hulun fault is a large porphyry copper-molybdenum deposit. Magmatic rocks are widespread in the mining area.

OBJECTIVES: In order to determine the emplacement age and tectonic setting of ore-hosting surrounding rock and ore-forming parent rock, and to discuss the petrogenesis and metallogenic dynamics.

METHODS: Zircon U-Pb isotopes and zircon Lu-Hf isotopes of rocks were studied by laser ablation multi-collector inductively coupled plasma mass spectrometry (LA-MC-ICP-MS) and laser ablation inductively coupled plasma-mass spectrometry (LA-ICP-MS).

RESULTS: (1) The zircons in the study area have a high content of REE with strong enrichment of HREE, δEu negative anomaly and δCe positive anomaly, and the REE distribution curves are left-inclined. (2) The anisomitic monzogranites are the ore-hosting rocks with a weighted average value of 200.96±0.88Ma, indicating that the rock mass was formed in early Jurassic. Zircon εHf(t) ranges from 0.1 to 5.8, single-stage Hf model ages (TDM) range from 643Ma to 882Ma, and two-stage Hf model ages (TDMC) range from 874Ma to 1235Ma. (3) The rhyolite porphyritic lavas are the ore-forming parent rocks with a weighted average value of 179.58±0.91Ma, indicating that the rocks formed in the Early Jurassic. Zircon εHf(t) ranges from 4.3 to 6.6, single-stage Hf model ages (TDM) range from 570Ma to 663Ma, and two-stage Hf model ages (TDMC) range from 802Ma to 952Ma.

CONCLUSIONS: The zircon Lu-Hf isotopic characteristics of the anisomitic monzogranites indicate that the magma source is a mixture of mantle and a small amount of ancient crust. The magma source area of the rhyolite porphyritic lavas is dominated by mantle-derived materials. The transition evolution process from crust source to mantle source from host rock to metallogenic parent rock is revealed.

KEY WORDS: Wunugetushan copper-molybdenum deposit; LA-MC-ICP-MS; U-Pb isotope; Lu-Hf isotope; petrogenesis